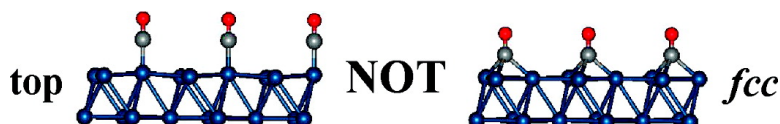


Successful a Priori Modeling of CO Adsorption on Pt(111) Using Periodic Hybrid Density Functional Theory

Yun Wang, Stefano de Gironcoli, Noel S. Hush, and Jeffrey R. Reimers

J. Am. Chem. Soc., **2007**, 129 (34), 10402-10407 • DOI: 10.1021/ja0712367 • Publication Date (Web): 02 August 2007

Downloaded from <http://pubs.acs.org> on February 15, 2009



More About This Article

Additional resources and features associated with this article are available within the HTML version:

- Supporting Information
- Links to the 4 articles that cite this article, as of the time of this article download
- Access to high resolution figures
- Links to articles and content related to this article
- Copyright permission to reproduce figures and/or text from this article

[View the Full Text HTML](#)

Successful a Priori Modeling of CO Adsorption on Pt(111) Using Periodic Hybrid Density Functional Theory

Yun Wang,[†] Stefano de Gironcoli,[‡] Noel S. Hush,[§] and Jeffrey R. Reimers^{*†}

Contribution from the School of Chemistry and School of Molecular and Microbial Biosciences, The University of Sydney, NSW 2006, Australia, and SISSA-Scuola Internazionale Superiore di Studi Avanzati and CNR-INFM DEMOCRITOS National Simulation Center, I-34014 Trieste, Italy

Received February 21, 2007; E-mail: reimers@chem.usyd.edu.au

Abstract: The adsorption of CO on the surface of metals such as Pt(111) is of great interest owing to the industrial importance of the catalytic oxidation of pollutant CO. To date, reliable high-level calculations of this process have not been possible, a situation often referred to as the “CO/Pt(111) puzzle”. Standard generalized-gradient-approximation density functional theory approaches fail to capture key details of the binding, such as the location of the adsorption site, while cluster approaches using alternative methods show some but insufficient improvement. Using a new computational methodology combining hybrid density functionals containing non-local Hartree–Fock exchange with periodic imaging plane-wave-based techniques, we demonstrate that key aspects of the adsorption of CO on Pt(111), including the identification of the adsorption site and CO frequency change, can now be adequately modeled. The binding is dominated by both CO dative covalent bonding and metal-to-molecule π back-bonding, effects requiring realistic alignment of both the molecular HOMO and LUMO orbitals with respect to the metal Fermi energy.

1. Introduction

While application of density functional theory (DFT) using the generalized gradient approximation (GGA) for the exchange–correlation functional has delivered significant achievements in studies of surface phenomena, key properties of some reactions, including the adsorption of CO on the Pt(111) surface, are not reproduced.¹ Such failures are significant, however, as the adsorption of CO on the metallic surface is the first step to its catalytic oxidation, an important industrial process that reduces the pollution produced by internal combustion and other engines. Indeed, this process is regarded as a prototypical system for the study of molecular–surface interactions; the adsorption properties have been extensively studied both theoretically and experimentally.^{1–8} Low-energy electron diffraction (LEED) and electron energy loss spectroscopy (EELS) results show that CO adsorbs at low coverage in a $(\sqrt{3} \times \sqrt{3})\text{-R}30^\circ$ structure and resides on the top site of the Pt(111) surface.² Contrary to these

experimental findings, GGA-based DFT predicts that the CO molecule adsorbs on the three-fold face-centered cubic (fcc) site.¹ Some factors that can affect the accuracy of computations, such as variations of the GGA exchange–correlation functional, computational implementations used in different program packages, defects, dopant, coverage, zero-point energies and vibrational corrections, spin-polarization, and relativistic correction, have been carefully excluded and shown not to be able to account for the discrepancy.¹ Similar phenomena are also observed in the adsorption of CO on the other metallic surfaces, indicating that this is a general issue in need of a widely applicable solution, an effect that has been described as the “CO/Pt(111) puzzle”.^{9,10}

Several theoretical studies have been performed to explain the CO/Pt(111) puzzle.^{6–8} Recent DFT studies by Kresse and co-workers showed that a linear relationship exists between the difference of the top and hollow site chemisorption energies for CO on Pt(111) and the gas-phase energy of the lowest unoccupied molecular orbital (LUMO) of the CO molecule.⁷ Also, Mason et al.⁸ have found a linear relationship between the top–hollow adsorption energy difference and the CO singlet–triplet excitation energy. Since the CO singlet–triplet excitation energy is closely related to the highest occupied molecular orbital (HOMO)–LUMO energy gap and hence the energy of the LUMO, these results suggest that the GGA functionals fail to properly balance the CO-to-metal dative-bonding interactions of the HOMO with the CO back-bonding

[†] School of Chemistry, The University of Sydney.

[‡] SISSA and CNR-INFM DEMOCRITOS.

[§] School of Molecular and Microbial Biosciences, The University of Sydney.

- (1) Feibelman, P. J.; Hammer, B.; Norskov, J. K.; Wagner, F.; Scheffler, M.; Stumpf, R.; Watwe, R.; Dumesic, J. *J. Phys. Chem. B* **2001**, *105*, 4018.
- (2) Steininger, H.; Lehwald, S.; Ibach, H. *Surf. Sci.* **1982**, *123*, 264.
- (3) Schweizer, E.; Persson, B. N. J.; Tushaus, M.; Hoge, D.; Bradshaw, A. M. *Surf. Sci.* **1989**, *213*, 49.
- (4) Blackman, G. S.; Xu, M. L.; Ogletree, D. F.; Vanhove, M. A.; Somorjai, G. A. *Phys. Rev. Lett.* **1988**, *61*, 2352.
- (5) Alavi, A.; Hu, P. J.; Deutsch, T.; Silvestrelli, P. L.; Hutter, J. *Phys. Rev. Lett.* **1998**, *80*, 3650.
- (6) Gil, A.; Clotet, A.; Ricart, J. M.; Kresse, G.; Garcia-Hernandez, M.; Rosch, N.; Sautet, P. *Surf. Sci.* **2003**, *530*, 71.
- (7) Kresse, G.; Gil, A.; Sautet, P. *Phys. Rev. B* **2003**, *68*.
- (8) Mason, S. E.; Grinberg, I.; Rappe, A. M. *Phys. Rev. B* **2004**, *69*, 161401(R).

- (9) Moler, E. J.; Kellar, S. A.; Huff, W. R. A.; Hussain, Z.; Chen, Y. F.; Shirley, D. A. *Phys. Rev. B* **1996**, *54*, 10862.
- (10) Gajdos, M.; Hafner, J. *Surf. Sci.* **2005**, *590*, 117.

interactions of the LUMO. As GGA functionals generally position the HOMO orbital well but underestimate the HOMO–LUMO gap, overestimation of the back-bonding interactions has been postulated as the generic solution to the CO/Pt puzzle.^{7,8} The suggestion that these bonding effects need to be properly treated originates actually from the 1964 Blyholder model¹¹ for chemisorbed CO, a model whose basic applicability is verified by these studies.

The failure of GGA functionals to correctly predict molecular HOMO–LUMO gaps is a problem of significant current interest, and many approaches have been suggested. Of these, one method known as “DFT+U” has already been applied to the CO/Pt puzzle.^{7,12} This approach introduces an empirical parameter, U , that is related to the screened coulomb and exchange integrals, with the value of U set so as to achieve agreement of the calculated HOMO–LUMO gap with experimental results. Another empirical approach that has also been used is to introduce computed CO singlet–triplet excitation energies obtained from high-level coupled-cluster and configuration-interaction (CI) quantum chemical computations to correct the adsorption energy.⁸ However, neither of these approaches was found capable of directly resolving the CO/Pt(111) puzzle.

The intrinsic origin of the underestimated HOMO–LUMO energy gaps comes from the core approximations used in generating GGA functionals. According to the quantum mechanism, the exact exchange–correlation (XC) functional is a truly non-local quantity that depends on the electronic density in two different points.¹³ However, most density functionals used in current DFT approximate the non-local XC functional with either purely local (the local density approximation, LDA) or semi-local (GGA and the later meta-GGA) functionals.¹⁴ In addition, the use of independent exchange and correlation functionals leads to a general self-interaction error in DFT: for an electron interacting with itself, these two contributions should exactly cancel, but as the functionals are independent, cancellation is incomplete and a significant error in calculated HOMO energy levels results. The result is that it is quite difficult for GGA and related functionals to properly balance dative-bonding and back-bonding interactions of metals with bifunctional ligands such as CO. An alternative approach designed specifically to deal with these issues in an a priori manner is hybrid DFT, in which a component of Hartree–Fock exchange is included into the density functional.^{15–17} While some pure GGA functionals can achieve results as accurate or more accurate than those that have been produced by hybrid functionals, the enhanced treatment of the fundamental processes embodied within the hybrid functionals makes them more robust and the functionals of choice in chemical applications of DFT,^{18,6} with the exception of applications in molecular electronics.¹⁹

To date, hybrid functionals have only been available on a widespread basis for use in calculations of non-periodic molecular systems. Processes on surfaces may be studied by such means through the introduction of cluster models of the surface, but these are limited somewhat, as very large clusters are typically required.^{6,20,21} One hybrid HF/DFT study investigating the CO/Pt(111) system has been performed using a cluster model.¹⁵ This led to the conclusion that the fcc site remains the most energetically favorable site, contrary to experiment. However, the energy difference between the fcc site and the top site is greatly reduced after employing the hybrid B3LYP functional,¹⁵ leading to the postulate that hybrid functionals may correctly describe the chemical processes if a complete periodic description of the solid is used. In this work we examine this hypothesis, making use of recent computational advances that allow for the use of hybrid functionals in periodic systems using plane-wave basis sets.^{22–25}

2. Computational Details

All the computations are performed by using the Quantum-ESPRESSO program.²⁶ The hybrid PBE0 XC functional is employed,¹⁷ along with the Perdew–Burke–Ernserhof (PBE) GGA from which it is derived;²⁷ only one parameter is included in order to add Hartree–Fock exchange to PBE, with

$$E^{\text{PBE0}} = \alpha E^{\text{exx}} + (1 - \alpha) E_{\text{PBE}}^{\text{x}} + E_{\text{PBE}}^{\text{c}} \quad (1)$$

where E^{exx} is the Hartree–Fock exchange, and $E_{\text{PBE}}^{\text{x}}$ and $E_{\text{PBE}}^{\text{c}}$ are the exchange and correlation energies using the PBE GGA functional, respectively. The parameter α is optimized to 0.25 for PBE0.¹⁷

Electron–ion interactions are described using relativistic norm-conserving pseudopotentials. Since no suitable pseudopotential database has been developed that is optimized for the PBE0 functional, the s^1d^9 PBE pseudopotential, obtained by using the FHI98PP package,²⁸ is utilized for all atoms. A plane-wave cutoff energy of 70 Ry (952 eV) is used throughout. The Pt bulk properties are calculated with the $(8 \times 8 \times 8)$ Monkhorst–Pack k -point mesh for integration over the Brillouin zone and one auxiliary $(8 \times 8 \times 8)$ k -point mesh for the calculation of E^{exx} . For a $(\sqrt{3} \times \sqrt{3})$ -R30° surface, the $(4 \times 4 \times 1)$ Monkhorst–Pack k -point mesh is used, and the auxiliary $(4 \times 4 \times 1)$ k -point mesh is used for the calculation of E^{exx} . For the calculation of the fractional occupancies, a broadening approach proposed by Methfessel and Paxton is used with an electronic temperature of 0.27 eV. The Pt(111) surface is modeled by a four-layer slab and a seven-layer-thick vacuum region that forms a three-dimensional periodic structure. On optimization, the top two layers and the adsorbate are allowed to relax, with the remaining substrate atoms being fixed at their bulk-like structure. Given that GGA computations describe the structural properties of the CO–Pt surface adequately,¹⁴ only single-point energy calculations are performed using PBE0 at PBE-optimized coordinates. For reference, additional calculations are performed using the Ceperley–Alder (CA) LDA,²⁹ the PBE GGA,²⁷ and the Perdew–Wang (PW91)³⁰ GGA functional.

- (11) Blyholder, G. J. *Phys. Chem.* **1964**, *68*, 2772.
 (12) Dudarev, S. L.; Botton, G. A.; Savrasov, S. Y.; Humphreys, C. J.; Sutton, A. P. *Phys. Rev. B* **1998**, *57*, 1505.
 (13) Baerends, E. J.; Gritsenko, O. V. *J. Phys. Chem. A* **1997**, *101*, 5383.
 (14) Kohanoff, J. *Electronic structure calculations for solids and molecules*; Cambridge University Press: Cambridge, 2006.
 (15) Becke, A. D. *J. Chem. Phys.* **1993**, *98*, 5648.
 (16) Stephens, P. J.; Devlin, F. J.; Chabalowski, C. F.; Frisch, M. J. *J. Phys. Chem.* **1994**, *98*, 11623.
 (17) Adamo, C.; Barone, V. *J. Chem. Phys.* **1999**, *110*, 6158.
 (18) Zhao, Y.; Pu, J. Z.; Lynch, B. J.; Truhlar, D. G. *Phys. Chem. Chem. Phys.* **2004**, *6*, 673.
 (19) Solomon, G. C.; Reimers, J. R.; Hush, N. S. *J. Chem. Phys.* **2004**, *121*, 6615.

- (20) Bilic, A.; Reimers, J. R.; Hoft, R. C.; Ford, M. J. *J. Comput. Theor. Chem.* **2006**, *2*, 1093.
 (21) Solomon, G. C.; Reimers, J. R.; Hush, N. S. *J. Chem. Phys.* **2005**, *122*, 224502.
 (22) Gygi, F.; Baldereschi, A. *Phys. Rev. B* **1986**, *34*, 4405.
 (23) Paier, J.; Marsman, M.; Hummer, K.; Kresse, G.; Gerber, I. C.; Angyan, J. G. *J. Chem. Phys.* **2006**, *124*, 154709; **2006**, *125*, 249901 (erratum).
 (24) Sorouri, J.; Foulkes, W. M. C.; Hine, N. D. M. *J. Chem. Phys.* **2006**, *124*, 064105.
 (25) Stadele, M.; Moukara, M.; Majewski, J. A.; Vogl, P.; Gorling, A. *Phys. Rev. B* **1999**, *59*, 10031.
 (26) Baroni, S.; Dal Corso, A.; de Gironcoli, S.; Giannozzi, P.; Cavazzoni, C.; Ballabio, G.; Scandolo, S.; Chiarotti, G.; Focher, P.; Pasquarello, A.; Laasonen, K.; Trave, A.; Car, R.; Marzari, N.; Kokalj, A. *Quantum-ESPRESSO*, V3.1.1; <http://www.pwscf.org/>.
 (27) Perdew, J. P.; Burke, W.; Ernzerhof, M. *Phys. Rev. Lett.* **1996**, *77*, 3965.
 (28) Fuchs, M.; Scheffler, M. *Comput. Phys. Commun.* **1999**, *119*, 67.

Table 1. C–O Bond Length $d_{\text{C-O}}$, LUMO–HOMO Energy Gap $E_{\text{LUMO-HOMO}}$, and Atomization Energy E_{at} of the Isolated CO Molecule as Well as the Lattice Constant a and the Cohesive Energy E_{coh} of the Bulk Pt Calculated Using Various Exchange–Correlation Functionals

	CA	PW91	PBE	PBE0	expt
$d_{\text{C-O}}$ (Å)	1.14	1.14	1.14	1.13	1.13
$E_{\text{LUMO-HOMO}}$ (eV)	6.92	7.04	7.03	9.42	
E_{at} (eV)	−12.4	−11.4	−12.1	−11.1	−11.1
a (Å)	3.91	3.99	3.98	3.93	3.92
E_{coh} (eV)	−7.38	−5.45	−5.17	−6.09	−5.83

Single-point energy calculations are also used to estimate the vibration frequency of CO on the surface at the top site. Only the Pt–C and C–O stretching coordinates are used in these calculations; inclusion of both coordinates is essential, as coordination of C to the surface decreases the effective mass of the C atom, thus increasing the CO vibration frequency without perturbing the CO force constant. This step also results in the determination of an optimized CO bond length for the PBE0 density functional.

3. Results and Discussion

3.1. Isolated CO Molecule. First, the properties of the isolated CO molecule are investigated to check the validity of the hybrid HF/DFT method. The calculated C–O bond length, HOMO–LUMO gap energy, and atomization energy are listed in Table 1, along with the corresponding CA, PBE, and PW91 results as well as the appropriate experimental data.³¹ While all of the calculations predict accurate C–O bond lengths and atomization energies, large variations are found for the HOMO–LUMO gap: PBE0 predicts a gap that is larger by at least 2 eV than those predicted by the other methods. The densities of states (DOSs) of the isolated CO molecule are presented in Figure 1, calculated using both the PBE and PBE0 functionals. This figure shows that the PBE0 HOMO energy is −10.01 eV, 1.61 eV lower than the corresponding PBE value, while the PBE0 LUMO locates at −0.60 eV, 0.77 eV higher than the PBE LUMO energy. Inclusion of the contribution from Hartree–Fock exchange thus has the desired effects of stabilizing the HOMO level and destabilizing the LUMO, attributable to the anticipated reduction of the DFT self-interaction energy error.

The numerically calculated CO vibration frequencies are 2179 cm^{-1} using PBE and 2258 cm^{-1} using PBE0, decreasing to 2125 and 2217 cm^{-1} , respectively, after anharmonic correction, close to the observed³² value of 2143 cm^{-1} . Obtained using GAUSSIAN 03³³ without the use of the pseudopotential approximation, the calculated PBE harmonic vibration frequency is 2128 cm^{-1} , using either the aug-cc-pVQZ or aug-cc-pV5Z basis set,³⁴ and hence the effect of the pseudopotential is seen to introduce a 51 cm^{-1} shift in the harmonic vibration frequency. The vibrational properties of CO, including its vibrational Stark effect, have been extensively studied in benchmark calculations.³⁵

3.2. Properties of Pt Bulk and the Pt(111) Surface. Some properties of bulk Pt calculated using the various XC functionals

are also listed in Table 1, with our results for the LDA and GGA functionals being very similar to those previously reported.³⁶ The lattice constant is overestimated by 1.6% using PBE and PW91, but, due to a fortuitous error cancellation, the CA LDA value is very close to experiment; PBE0 also predicts the correct lattice parameter. For the cohesive energy, the difference of the average energy of the bulk Pt atom and the total energy of an isolated Pt atom, CA overbinds³⁷ by 1.55 eV, while the GGAs underbind by 0.38–0.66 eV; PBE0 overestimates the cohesive energy by 0.26 eV, providing the closest prediction to the experimental value.

The calculated 5d-band DOSs of the bulk Pt are also presented in Figure 1. Inclusion of Hartree–Fock exchange is seen to broaden the 5d band and open up a small band gap at the Fermi energy; while this band broadening is likely to be a physically realistic effect, the introduced band gap is an artifact that arises from the exclusion of true non-local correlation for the PBE0 functional. Finally, Figure 1 also shows the 5d surface-atom DOS, revealing effects similar to those found for bulk atoms. This artifact will be of consequence for any calculated physical property based on the DOS at the Fermi energy, and it is this effect that has, in general, restricted the use of hybrid functionals in calculations involving conductors. However, the interaction of the metal with adsorbates is not affected by the presence of this band gap, as chemical interaction energies are typically an order of magnitude larger than the introduced error. This effect is responsible for the widespread success of cluster models for the chemistry of molecule–metal interactions, approaches that induce much larger band gaps than are here manifested.

3.3. Adsorption Properties of CO on Pt(111). The energy of adsorption of CO on Pt(111) at various sites obtained using the PBE and PBE0 functionals is given in Table 2; the PBE results are in agreement with previous calculations,^{1,6} and the adsorption energy is defined as

$$\Delta E_{\text{ad}} = E_{\text{tot}} - E_{\text{surf}} - E_{\text{CO}} \quad (2)$$

where E_{tot} and E_{surf} are the optimized total energies of the systems with and without adsorbate, respectively, and E_{CO} represents the energy of the isolated CO molecule. As has been widely noted for GGA functionals, PBE predicts incorrectly that the fcc site is the most stable site. The adsorption energy at the fcc site is calculated to be −1.64 eV, close to that calculated using the PAW method with the same functional, indicating that the choice of pseudopotential is not critical.⁶ Also, the PBE-calculated relative energy of 0.11 eV for the top site, along with the calculated CO bond lengths, are in good agreement with previous results.^{1,6} These results show that our computation details, such as the slab thickness, cutoff energy, and k -point mesh, are good enough to produce reliable results.

The single-point energies obtained using PBE0 at the PBE-optimized geometries given in Table 2 predict quite a different scenario: the calculated energy of adsorption at the top site of −1.80 eV is close to the experimental results of −1.41 to −1.73 eV.² Also, this value is 0.13 eV lower than that calculated at the fcc site, in agreement with the observed site preference.^{2,3} The calculated differences between the results of the PBE0 and

(29) Ceperley, D. M.; Alder, B. J. *Phys. Rev. Lett.* **1980**, *45*, 566.

(30) Perdew, J. P.; Wang, Y. *Phys. Rev. B* **1992**, *45*, 13244.

(31) Huber, K. P.; Herzberg, G. *Molecular spectra and molecular structure. IV. Constants of diatomic molecules*; Van Nostrand Reinhold Co.: New York, 1979.

(32) Herzberg, G. *Molecular spectra and molecular structure. I. Spectra of diatomic molecules*, 2nd ed.; Van Nostrand: Princeton, 1965.

(33) Frisch, M. J.; et al. *GAUSSIAN 03*, Revision B2; Gaussian Inc.: Pittsburgh, PA, 2003.

(34) Woon, D. E.; Dunning, T. H., Jr. *J. Chem. Phys.* **1993**, *98*, 1358.

(35) Reimers, J. R.; Hush, N. S. *J. Phys. Chem. A* **1999**, *103*, 10580.

(36) Pushpa, R.; Narasimhan, S. *Bull. Mater. Sci.* **2003**, *26*, 91.

(37) Kittel, C. *Introduction to solid state physics*, 5th ed.; Wiley & Sons: New York, 1976.

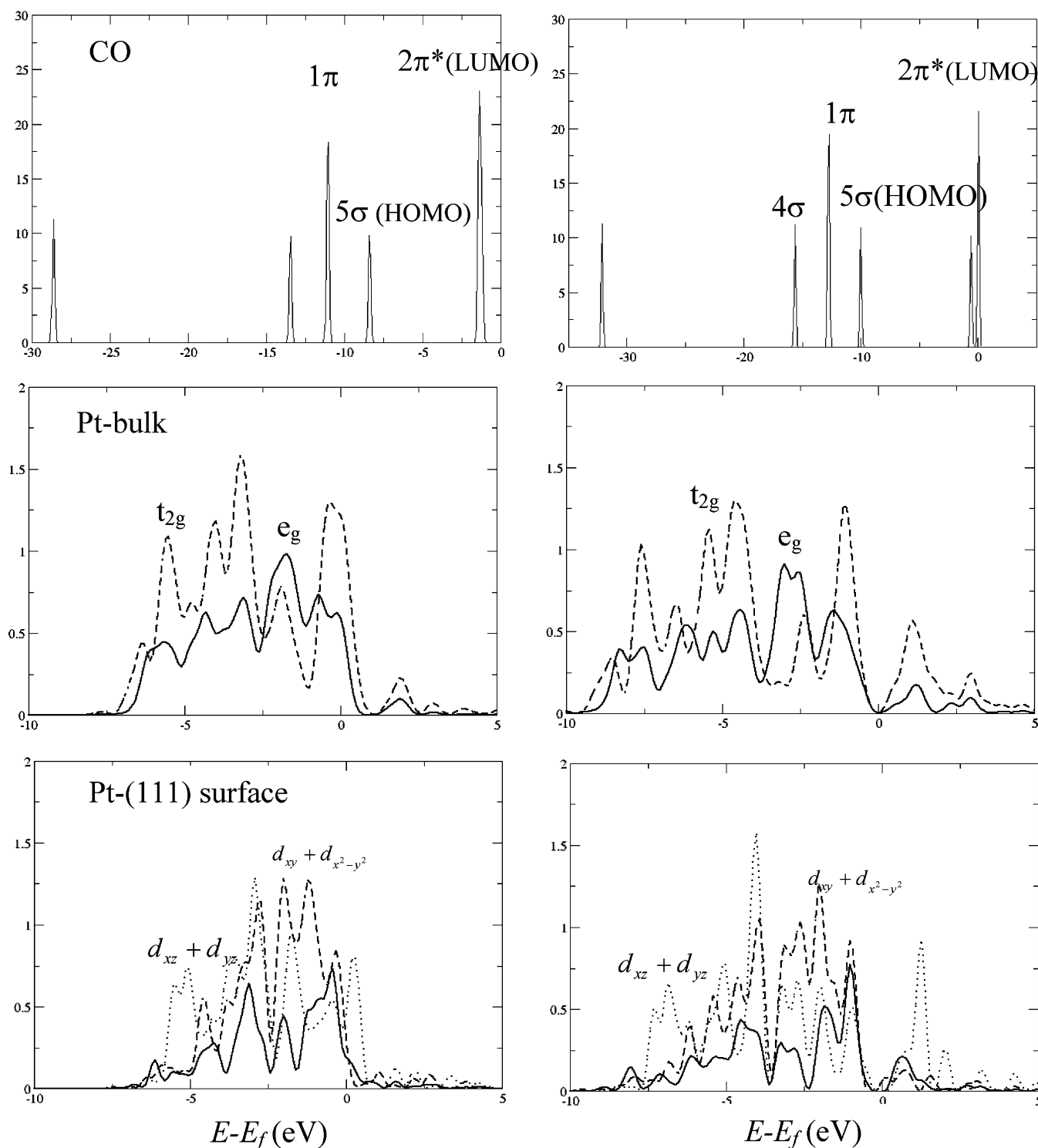


Figure 1. Densities of states of the isolated CO molecule, and the orbital-resolved density of states bulk and Pt(111) surface atoms, calculated using (left) PBE and (right) PBE0.

Table 2. Energy of Adsorption (eV) of the CO Molecule on the Pt(111) ($\sqrt{3} \times \sqrt{3}$)-R30° Surface at Different Sites, Obtained Using the PBE and PBE0 Functionals at PBE-Optimized Geometries

	fcc	bridge	top
PBE	-1.64	-1.61	-1.53
PBE0	-1.67	-1.68	-1.80

PBE calculations arise as PBE0 predicts stronger binding at the top site by 0.27 eV and stronger binding at the fcc site by just

0.03 eV. Previous attempts at enhancing results from GGA calculations by simply adjusting the LUMO level through the DFT+U^{7,12} or triplet-energy correction methods⁸ predicted weaker binding in comparison with the PBE results. Hence, it is clear that these empirical approaches only recover some of the effects of the non-local nature of the exchange interaction, attributable to their correction of only the LUMO energy instead of correction of both the HOMO and the LUMO energies apparent from Figure 1.

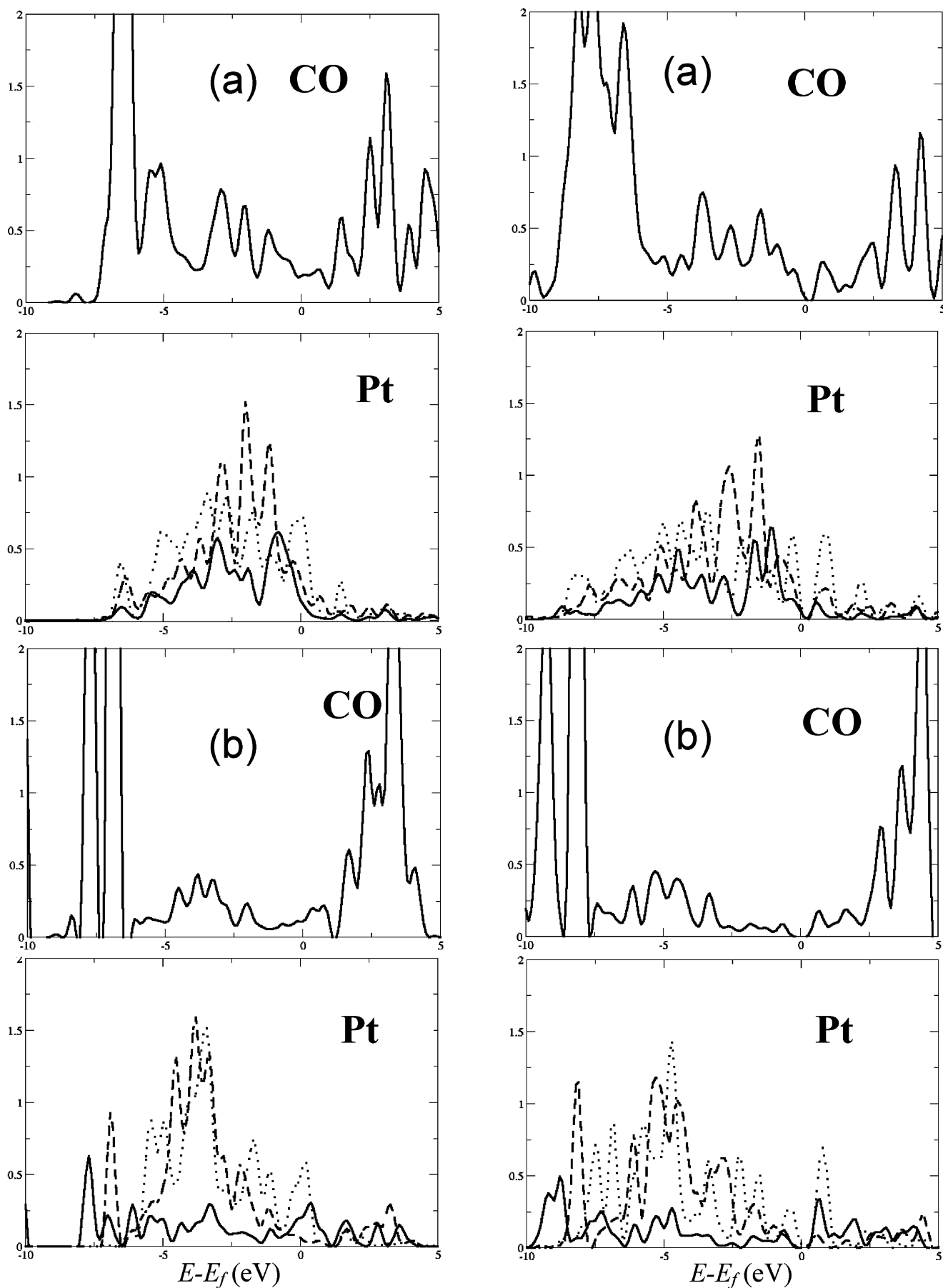


Figure 2. Partial densities of states of the CO molecule and the d orbitals of the Pt atom which is connected with the C atom obtained using PBE (left) and PBE0 (right): (a) the fcc site and (b) the top site. The solid line presents the DOS of d_z^2 , the dashed line is for $d_{xz} + d_{yz}$, and the dotted line is for $d_{xy} + d_{x^2-y^2}$.

Vibrational shifts for CO on top-site adsorption have been calculated numerically using a two-dimensional model involving the C–O and Pt–C stretch coordinates only. A shift of -6 cm^{-1} is predicted using PBE, compared to -26 cm^{-1} predicted using PBE0 and an observed shift³ of -39 cm^{-1} . However, coordination of the C atom to the surface changes the effective mass of the atom,³⁸ increasing the CO frequency by 40 cm^{-1} ; hence, the perceived changes to the CO frequency arising from changes to the CO force constant are -46 and -66 cm^{-1} for PBE and PBE0, respectively. The effects of adsorption on the structure of CO predicted by PBE0 are thus 50% larger than those predicted by PBE. Much effort has been put into understanding the physical aspects of these effects.^{11,38–42} Our calculations also provide a crude estimate of the Pt–C vibration frequency. This is determined to be 530 cm^{-1} , close to the observed value³⁹ of 480 cm^{-1} .

3.4. The Role of Non-local Exchange in Determining the Binding. To understand the role of the non-local exchange, a study of the orbital-resolved DOSs at the top and fcc sites has been performed using both PBE and PBE0, and the results are shown in Figure 2; for the PBE functional, these results are similar to those previously reported.⁷ The states may be roughly divided into three energy regions. At low energies of -10 to -5 eV , there are signs of a CO- 5σ to Pt- $5d$ interaction, as well as a CO- 1π to Pt- d_{xz}/d_{yz} interaction. In the medium energy range of -5 to 0 eV , the CO $d\pi$ orbital⁴³ is apparent, indicating partial back-donation of electrons from the substrate to the originally empty CO molecular $2\pi^*$ orbital, the LUMO of the isolated molecule. Finally, at higher energies of 0 to 5 eV , the remnant character of the CO- $2\pi^*$ orbital appears.

Most significant, however, are the changes in these DOSs associated with bonding on the top and fcc sites. When the CO adsorbs at the fcc site, the CO- 5σ peaks shift to higher energy with respect to the corresponding peaks for the top site, indicating that the CO- 5σ to Pt- $5d$ interaction is weakened at the fcc site and donation from the adsorbate to surface is reduced. This weaker interaction is also indicated by longer Pt–C bond lengths at the fcc site. Concurrently, the CO- 5σ orbital interacts mainly with the Pt- d_{xy} or Pt- $d_{x^2-y^2}$ states at the fcc site, and with the Pt- $5d_{z^2}$ states at the top site (this can be understood by considering the symmetries of the adsorbed geometries). In the medium energy range, the $d\pi$ bands are more occupied at the fcc site, implying that, for this site, there is a *stronger* back-donation from the substrate to the CO antibonding orbital. Thus, two main interactions of the CO binding with the surface are identified: donation from the CO- 5σ to the substrate $5d$ orbital, and back-donation from the substrate to the CO LUMO orbital. The CO electron-donation process, which is sensitive to the location of the HOMO level, favors the top

site, while the back-donation process, which is sensitive to the location of the LUMO level, favors the fcc site. Hence, comparing the results obtained using the PBE and PBE0 functionals, it is clear that the corrections introduced through the use of non-local exchange to the HOMO and LUMO levels both contribute to the relative binding energies of the top and fcc sites, not just the LUMO energy as has been previously presumed.^{7,8,12}

4. Conclusions

The CO/Pt(111) puzzle associated with the failure of GGA-type functionals to properly describe the paradigm of CO adsorption to metals has been resolved using hybrid density functional theory implemented using periodic boundary conditions and a plane-wave basis set. Our results confirm that the incorrectly predicted CO LUMO level is a key contributor to the failure of GGA approaches,^{7,8} and this result is extended to show that correct positioning of the CO HOMO level is of equal importance. Indeed, the CO HOMO–LUMO energy gap obtained with the hybrid PBE0 functional is about 2 eV larger than that obtained when using the corresponding PBE GGA, with the error roughly equally distributed between the HOMO and LUMO. As anticipated, back-bonding from the substrate to the antibonding CO $2\pi^*$ LUMO, which is the main contribution to the adsorption energy at the fcc site, is greatly weakened by introducing the non-local exact exchange functional; however, dative bonding between the CO HOMO and the Pt $5d$ states is significant, and non-local exchange also affects this term to increase the preference for the top site. Thus, the top site is demonstrated to be the most energetically favorable site for CO adsorption on the flat Pt(111) surface. Proper balancing of these two types of bonding is also shown to be critical to the determination of the CO vibrational frequency shift on adsorption.

The catalysis of oxidation of CO on metal surfaces is a process of great significance to the control of environmental pollution, the study of which has previously been hampered by inadequate treatment of the electron-donation and back-donation processes by GGA functionals, coupled with the poor convergence of cluster-based approaches. The advent of new computational methods that properly describe the surface chemistry will open up this field of catalysis to high-level computation. However, the computation time with the hybrid DFT functional is hundreds to thousands of times longer than that using the simple GGA functionals. Further computational developments, such as the use of screened hybrid functionals,⁴⁴ will reduce this computation time, making useful calculations more feasible.

Acknowledgment. We thank the Australian Research Council for funding this work under the Discovery Grant program. The use of the supercomputer facilities at the Australia Partnership for Advanced Computing (APAC) is gratefully acknowledged.

Supporting Information Available: Complete ref 33. This material is available free of charge via the Internet at <http://pubs.acs.org>.

JA0712367

(38) Hush, N. S.; Williams, M. L. *J. Mol. Spectrosc.* **1974**, *50*, 349.

(39) Baro, A. M.; Ibach, H. *J. Chem. Phys.* **1979**, *71*, 4812.

(40) Koper, M. T. M.; van Santen, R. A.; Wasileski, S. A.; Weaver, M. J. *J. Chem. Phys.* **2000**, *113*, 4392.

(41) Bagus, P. S.; Muller, W. *Chem. Phys. Lett.* **1985**, *115*, 540.

(42) Bauschlicher, J.; Charles, W.; Bagus, P. S. *J. Chem. Phys.* **1984**, *81*, 5889.

(43) Fohlsch, A.; Nyberg, M.; Hasselstrom, J.; Karis, O.; Pettersson, L. G. M.; Nilsson, A. *Phys. Rev. Lett.* **2000**, *85*, 3309.

(44) Heyd, J.; Scuseria, G. E.; Ernzerhof, M. *J. Chem. Phys.* **2003**, *118*, 8207.